Highly Productive Propane Dehydrogenation Catalyst Using Silica-Supported Ga-Pt Nanoparticles Generated from Single-Sites

Author(s):
Searles, Keith; Chan, Ka Wing; Mendes Burak, Jorge A.; Zemlyanov, Dmitry; Safonova, Olga, V; Copéret, Christophe

Publication date:
2018-09-19

Permanent link:
https://doi.org/10.3929/ethz-b-000294420

Originally published in:
Journal of the American Chemical Society 140(37), https://doi.org/10.1021/jacs.8b05378

Highly Productive Propane Dehydrogenation Catalyst Using SilicaSupported Ga−Pt Nanoparticles Generated from Single-Sites

Keith Searles,† Ka Wing Chan,† Jorge Augusto Mendes Burak,† Dmitry Zemlyanov,§ Olga Safonova,‡ and Christophe Copéret *,†

† ETH Zürich, Department of Chemistry and Applied Biosciences, Vladimir Prelog Weg 1-5, ETH Zürich, CH-8093 Zurich, Switzerland

‡ Paul Scherrer Institut, CH-5232 Villigen, Switzerland

§ Birck Nanotechnology Center, Purdue University, 1205 West State Street, West Lafayette, Indiana 47907, United States

The development of more effective alkane dehydrogenation catalysts is a key technological challenge for the production of olefins from shale gas, an abundant source of light hydrocarbons. Surface organometallic chemistry provides an original approach to generate nanometric Ga−Pt bimetallic particles supported on partially dehydroxylated silica containing gallium single-sites, which displays high activity, selectivity, and stability in propane dehydrogenation. This catalyst was prepared via sequential grafting of a platinum precursor onto silica possessing site-isolated gallium sites followed by H2 reduction. Monitoring generation of the reduced species, Gaδ+ Pt0 /SiO2, via in situ X-ray absorption spectroscopy reveals formation of a GaxPt ($0.5 < x < 0.9$) alloy with a fraction of gallium remaining as isolated sites. This bimetallic material exhibits catalytic performance that far surpasses each of the individual components and other reported Ga−Pt based catalysts; this is attributed to the highly dispersed GaxPt alloyed structure on a support with low Brønsted acidity containing gallium single-sites.

A change of feedstock from naphta to light alkanes, due to the emergence of shale gas and the increasing availability of natural gas, has led to a decreased production of light olefins such as propene from cracking. This shift has directed major efforts in developing on-purpose alkane dehydrogenation technologies.1−4 Dehydrogenation of lightweight alkanes is an extremely energy intensive process largely due to a high positive enthalpy of the reactions (ΔrH° = 137 and 124 kJ mol−1 for C2H6 and C3H8, respectively), necessitating high reaction temperatures. Consequently, the operating conditions present major challenges for catalyst stability and selectivity. The primary industrial technologies operated for direct propane dehydrogenation (PDH) are CrO3/Al2O3 (CB&I Lummus Catofin process) and Pt−Sn/Al2O3 (Oleflex process). Both catalysts suffer from rapid deactivation and require frequent regeneration as often as 15−20 min for the industrial chromium catalysts.2−6 Hence, the development of more stable and robust catalysts with less frequent regeneration cycles is currently of major research interest. A strategy to develop more stable platinum catalysts has relied on the preparation of bimetallic systems that include various promoter elements (e.g., Cu, Zn, Ga, In, Ge, Sn, etc.) to enhance the stability and selectivity of platinum in PDH. A notable bimetallic combination is Ga−Pt, where each individual component can be active in PDH but typically suffers from lower activity and facile deactivation when used separately.2,7,8 The primary preparation method for bimetallic Ga−Pt catalysts, and others, has relied on sequential impregnations of oxide supports,9−12 including modifiedhydrotalictes,13−19 followed by a reduction step yielding reduced surface species. While synthetically straightforward and yielding improved catalytic performances, these approaches have led to difficulty in identifying the active sites due to low quantities of active species associated with the presence of large amounts of bulk species. This ultimately hinders a fundamental understanding of the active site and rational improvement of the catalysts. In the case of Ga−Pt catalysts, the improved activity has largely been attributed to the formation of Ga−Pt alloyed particles with platinum serving as the active site and gallium as a promoter.9,11,15,16,18 However, alternative assignments have suggested Ga2O3- domains to be active where small quantities of platinum particles facilitate H2 removal from the Ga2O3 surface.10,12 While the exact nature of the active sites still remains to be determined, the controlled development of well-

defined multicomponent heterogeneous systems that possess long term stability remains both a promising avenue for catalyst design and a synthetic challenge. An alternative approach for developing well-defined PDH catalysts has relied on the synthesis of single-site catalysts, either prepared through electrostatic adsorption methods20−24 or through a two-step approach combining surface organometallic chemistry (SOMC)25−29 and the thermolytic molecular precursor approach (TMP).30 We have previously developed several single-site catalysts, M/SiO2 (M = CrIII, CoII, and GaIII), for PDH using the latter strategy.31−34 This approach generates isolated metal-sites along with isolated surface silanols, creating an opportunity to anchor other metal precursors and generate well-defined bimetallic systems containing supported metallic nanoparticles in the presence of additional isolated metal-sites.35−39 This provides means of tuning or enhancing chemical reactivity and selectivity of the catalytic systems as well as introducing unique stabilizing features for the nanoparticles. Herein, we describe the synthesis of a bimetallic Ga−Pt system prepared through grafting a platinum precursor onto the surface of silicasupported gallium single-sites. Following reduction under H2, nanometric Ga−Pt bimetallic particles are formed where a fraction of gallium remains as isolated surface-sites. These materials have been characterized by several spectroscopic techniques including X-ray photoelectron spectroscopy (XPS) and in situ X-ray absorption spectroscopy (XAS) studies monitoring the reduction process and catalysis. We show that this material is highly selective (≥99%) and active (31.5 g C3H6 g cat−1 h−1) under high WHSVs (ca. 100 g C3H8 g cat−1 h−1) at 550 °C, where equilibrium conversions are initially approached. After a 20 h catalytic test, the catalyst shows limited deactivation. The overall high catalytic performance combining high activity, selectivity, and stability in PDH is attributed to the combination of small alloyed Ga−Pt nanoparticles (ca. 1 nm) and a support with dispersed Lewis acidic gallium single-sites combined with low Brønsted acidity.

To prepare the bimetallic Ga−Pt system, the platinum precursor [Pt(OSi(OtBu)3)2(COD)]40,41 was grafted onto the surface of silica containing gallium single-sites prepared via SOMC,

[(≡SiO)3Ga(HOSi≡)] (GaIII/SiO2, 1.45 wt % Ga, 0.44 mmol OH g−1).34 The grafting resulted in the release of 0.9 equiv of HOSi(OtBu)3 per consumed platinum complex yielding a material with equimolar amounts of gallium and platinum (1.55 wt % Ga, 4.37 wt % Pt, Figure 1a). IR analysis of the colorless solid after washing and drying under high vacuum (10−5 mbar) indicated a partial disappearance of −OH vibrations and the appearance of νCH in the range of 3050− 2800 and 1490−1350 cm−1 . 13C MAS SSNMR measurements also support retention of −OSi(OtBu)3 and COD ligands at the surface (see Supporting Information for details), which is in agreement with elemental analysis (4.0 wt % C, 14.9 C atoms per platinum). These data are consistent with the presence of gallium single-sites and the grafted platinum species, namely, [(≡SiO)3Ga(HOSi≡)(≡SiO)Pt(OSi- (OtBu)3)(COD)] (GaIIIPtII/SiO2). The bimetallic system GaIIIPtII/SiO2 was then subjected to reduction at 500 °C under a flow of H2 at 1 atm for 12 h. IR analysis of the material after cooling to room temperature under vacuum (10−5 mbar) evidenced complete removal of organic ligands from the surface with concomitant restoration of surface silanols. After H2 treatment, the colorless material acquired a significantly darker color, indicative of particle formation. Transmission electron microscopy (TEM) confirmed the presence of nanometric particles with a narrow size distribution (1.0 ± 0.2 nm, Figure 1b). Elemental analysis performed on this material indicated a 0.85 molar ratio of Ga/Pt remaining on the material after reduction.

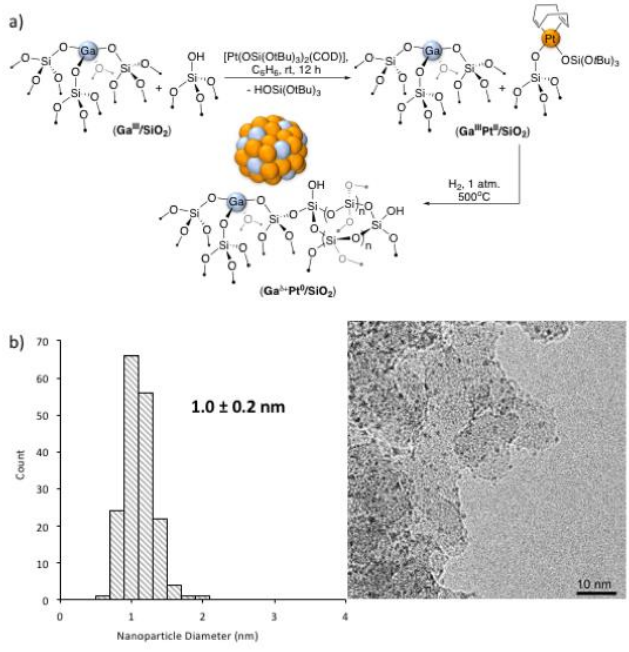

Figure 1. a) Synthesis of the bimetallic $\mathbf{Ga^{III}Pt^{II}/SiO_2}$ and $\mathbf{Ga^{\delta+}Pt^{0}/SiO_2}$ materials. b) Representative TEM image and particle size distribution of $\mathbf{Ga^{\delta+}Pt^{0}/SiO_2}$.

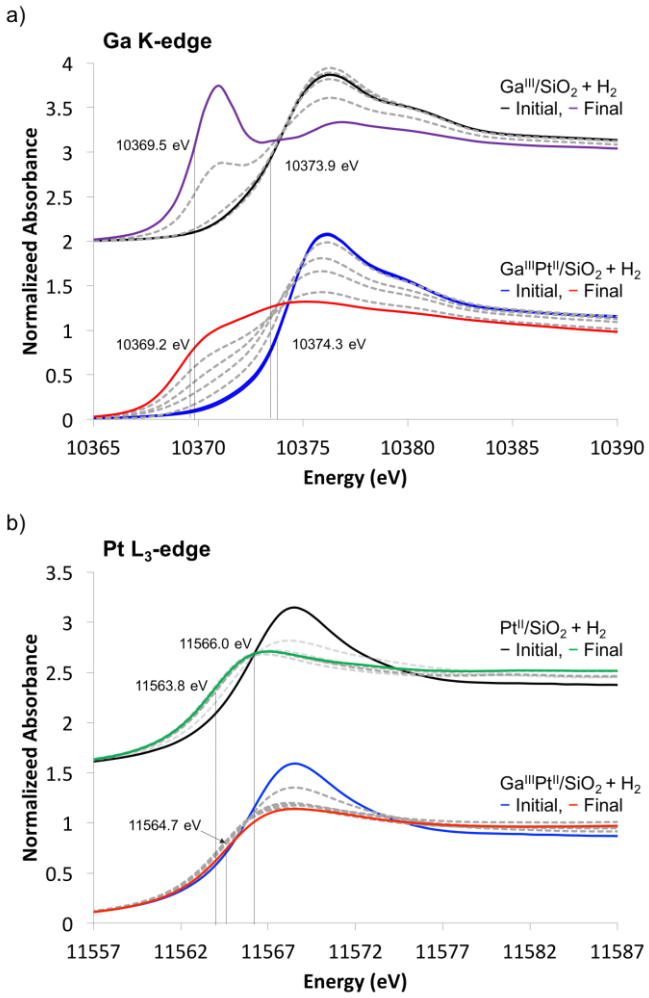

Figure 2. In situ XANES spectra at a) Ga K-edge for $\mathbf{Ga^{III}/SiO_2}$ (top) and $\mathbf{Ga^{III}Pt^{II}/SiO_2}$ (bottom) and b) Pt L_3-edge for $\mathbf{Pt^{II}/SiO_2}$ (top) and $\mathbf{Ga^{III}Pt^{II}/SiO_2}$ (bottom). Spectra were recorded under 1 atm of H_2 flow (10 mL/min) with subsequent heating to 550 °C. Solid spectra represent initial and final states. Dashed spectra were recorded during progressive heating to 550 °C. Vertical dashed lines represent edge energies of initial and final states.

The surface of the particles was further probed via CO adsorption and desorption studies. A self-supporting pellet of the reduced bimetallic system exposed to 12 mbar of CO at room temperature reveals a single vibrational band centered at 2069 cm−1 at full surface coverage. This value is significantly red-shifted in comparison to monometallic platinum nanoparticles, Pt0 /SiO2, prepared by SOMC, which exhibit a vibrational band centered at 2090 cm−1 obtained under the same conditions. Furthermore, these CO bands are red-shifted by 3 and 30 cm−1 at low coverage for the reduced GaPt system and Pt0 /SiO2, respectively, which evidence significant variation of the particle surfaces between these two systems; already indicating that the surface Pt atoms in the reduced GaPt material are likely isolated sites. Pyridine adsorption studies were also performed to investigate Lewis acidic surface sites. These studies reveal vibrational bands characteristic of pyridine adsorption at GaIII/SiO2 24,34 along with additional vibrational bands that are similar to those attributed to α-pyridyl, arising from pyridine adsorption on Pt{111}.42−44 These adsorption studies indicate that the nanoparticles formed during reduction differ significantly from Pt0 /SiO2 and that the SiO2 support still retains Lewis acidic surface sites. XPS measurements were also performed to investigate the atomic composition and state of each component in the reduced bimetallic material. These measurements confirm nearly equal atomic ratios of gallium and platinum in the reduced material (Ga 3d, 0.48%; Pt 4f7/2, 0.51%). The Pt 4f7/2 spectra contains a single peak at 71.6 eV; this is 0.3 eV higher in energy compared to the Pt 4f7/2 spectra of Pt0 /SiO2, which displays a single peak at 71.3 eV. The higher electron binding energy can be attributed to the formation of an intermetallic alloy during the reduction process, which was further investigated by examining the Ga 2p3/2 spectra. This shows an asymmetric peak, which was fitted with two peaks at 1119.0 and 1117.2 eV. The former peak contributes to ca. 10% of the signal and is similar to XPS measurements performed on GaIII/ SiO2 (1119.1 eV). This observation is in agreement with pyridine adsorption studies and is consistent with a fraction of gallium remaining as single-sites. The remaining gallium is represented by the second component of the fitting at 1117.2 eV. This peak is 1.8 eV lower in electron binding energy and is consistent with the presence of reduced Gaδ+ . Considering both the Pt 4f7/2 and Ga 2p3/2 XPS spectra, the reduction process yields a reduced material, Gaδ+ Pt0 /SiO2, containing nanometric bimetallic

GaxPty (x < y) particles along with a fraction of GaIII single-sites. Additional H2 and CO chemisorption experiments support the formation of a GaxPty alloy and show similar trends in comparison to PtGa/Al2O3 systems prepared by sequential impregnation (see Supporting Information for details).9

Table 1. EXAFS fit parameters of Pt L_3-edge and Ga K-edge spectra for selected samples.

Pt L_3-Edge			
Sample	Neighbor, N[b]	r[Å][c]	σ^2[Å^2][d]
[Pt(OSi(O*t*Bu)$_3$)$_2$(COD)]	O, 2.0*	2.00 ± 0.02	0.002 ± 0.001
	C, 4.0*	2.19 ± 0.01	0.002 ± 0.001
	C, 2.0*	3.04 ± 0.03	0.006 ± 0.003
	C, 2.0*	3.11 ± 0.03	0.006 ± 0.003
$Ga^{III}Pt^{II}/SiO_2$	O, 2.0*	2.02 ± 0.04	0.007 ± 0.004
	C, 4.0*	2.18 ± 0.03	0.007 ± 0.004
$Ga^{\delta+}Pt^0/SiO_2$	Ga, 2.8 ± 0.5	2.471 ± 0.005	0.0095 ± 0.0009
	Pt, 2.8 ± 0.7	2.701 ± 0.005	0.007 ± 0.001
Ga K-edge			
Sample	Neighbor, N[b]	r[Å][c]	σ^2[Å^2][d]
$Ga^{III}Pt^{II}/SiO_2$	O, 3*	1.79 ± 0.02	0.002 ± 0.005
	O, 1*	1.9 ± 0.1	0.002 ± 0.005
$Ga^{\delta+}Pt^0/SiO_2$	Pt, 2.9 ± 0.5	2.471 ± 0.005	0.0095 ± 0.0009

	O, 1.4 ± 0.4	1.77 ± 0.01	0.008 ± 0.003

[a] All samples were recorded in transmission mode. [b] Number of specified neighbors. [c] Distance to corresponding neighbor. [d] Debye-Waller factor. Fitting parameters at set values are indicated by *.

In attempts to gain a more detailed structural understanding of the reduced species, we monitored the reduction of GaIIIPtII/SiO2, as well as for the corresponding monometallic systems, by XAS. The X-ray absorption near-edge structure (XANES) spectra are shown in Figure 2. Prior to reduction, the XANES spectra of GaIIIPtII/SiO2 at the gallium K-edge and platinum L3-edge are similar to GaIII/SiO2 and [(≡SiO)- Pt(OSi(OtBu)3)(COD)] (PtII/SiO2) with edge energies of 10373.9 and 11566.0 eV, respectively. Upon treatment of GaIIIPtII/SiO2 to 550 °C under 1 atm of H2 (10 mL/min), a decrease in edge-energy at the gallium K-edge from 10374.3 to 10369.2 eV is observed. The profile and white line intensity varies significantly in comparison to the spectrum of GaIII/ SiO2 exposed to H2 flow (Figure 2a). The platinum L3-edge was also investigated during the reduction of GaIIIPtII/SiO2, indicating a decrease in energy from 11566.0 to 11564.7 eV and a decrease in the white line intensity, fully consistent with the reduction of platinum.13,14,45 This edge energy is slightly higher when compared to Pt0 /SiO2 obtained upon reduction of PtII/SiO2 (Figure 2b). Alloying of platinum and gallium results in a decreased white line intensity and an increased edge-energy for the platinum L3-edge. This is consistent with electron transfer from a metallic phase of gallium to the platinum 5d band and a positive shift in the central position of the platinum 5d valence band with respect to the Fermi level previously described in the literature.13,14,46,47 Modification of platinum's electronic structure is consistent with CO adsorption studies indicating a more electron-rich platinum surface (vide supra). The extended X-ray adsorption fine structure (EXAFS) data was then investigated; fits of the experimental data are summarized in Table 1. Fits of the gallium K-edge for the reduced material, Gaδ+ Pt0 /SiO2, required the inclusion of Ga− O (N = 1.4 ± 0.4, 1.77 Å) and Ga−Pt (N = 2.9 ± 0.5, 2.471 Å) scattering paths. The Ga−O coordination distance is similar to those in silica-supported four-coordinate gallium single-sites and is in agreement with XPS data that gallium single-sites are present in Gaδ+ Pt0 /SiO2 (vide supra). The number of O neighbors also suggests that

some gallium atoms of the alloyed GaxPty particles, evidenced by the Ga−Pt scattering path, are interacting with the SiO2 surface. The unsuccessful inclusion of Ga−Ga scattering paths from metallic gallium and Ga2O3 in the fit confirms the absence of these phases. Fits of the platinum L3-edge for Gaδ+ Pt0 /SiO2 required Pt−Pt (N = 2.8 ± 0.7, 2.701 Å) and Pt−Ga (N = 2.8 ± 0.5, 2.471 Å) scattering paths, which further support the formation of small GaxPty alloyed nanoparticles. The total number of neighbors around platinum (5.6 ± 0.9) is slightly higher than the estimated number of neighbors around gallium in the alloy. This indicates that the gallium has a higher probability of being located at the particle−support interface and/or at the surface of the nanoparticle. However, gallium has to be highly dispersed in the nanoparticle as the Ga−Ga scattering path could not be included in the fits. Based on the XPS and XAS data, we suggest the alloy composition of the nanometric particles to be GaxPt ($0.5 < x < 0.9$). The ability to stabilize these ultrasmall and narrowly distributed alloyed particles on silica can be attributed to the presence of remaining gallium surface sites, which provided highly Lewis acidic centers for particle nucleation and stabilization.

Table 2. Catalytic performance of $Ga^{\delta+}Pt^0/SiO_2$, Pt^0/SiO_2 and Ga^{III}/SiO_2 systems for PDH at 550 °C under flow conditions.

Catalyst	Time	Conv	Selec	WHSV	k_d [c]
$Ga^{\delta+}Pt^0/SiO_2$	0.3 h	31.9%	>99%	98 h^{-1} [a]	0.04
	20 h	17.1%	>99%		
$Ga^{\delta+}Pt^0/SiO_2$	0.3 h	40.7%	63.5%	2.0 h^{-1} [b]	0.01
	20 h	38.5%	70.1%		
Pt^0/SiO_2	0.3 h	19.0%	59.2%	2.2 h^{-1} [b]	1.0
	2.0 h	4.4%	46.1%		

Ga^{III}/SiO_2	0.3 h	9.3%	94.0%	2.1 h^{-1} [b]	0.02
	20 h	6.5%	93.0%		

[a] 50 mL/min; 20% C_3H_8 in Ar. [b] 10 mL/min; 20% C_3H_8 in Ar. [c] $k_d = (\ln(1-conv_{end}/conv_{end})-\ln(1-conv_{start}/conv_{start}))/t$, where $conv_{start}$ is the initial conversion, $conv_{end}$ is the final conversion, and t is the duration of the experiment expressed in hours.[2]

The catalytic performance of Gaδ+ Pt0 /SiO2 was then investigated for PDH at 550 °C under flow conditions (50 mL/min; 20% C3H8 in Ar; WHSV, 98.3 h−1). An initial propane conversion of 31.9% was achieved with >99% selectivity for C3H6 (Table 2). The high propylene selectivity (>99%) was maintained over the duration of the catalytic test (20 h), while reaching a final propane conversion of 17.1%. At lower flow rates (10 mL/min; 20% C3H8 in Ar; WHSV, 2.0 h−1) and longer residence times, propane conversion increases accompanied by a significant drop in selectivity, likely due to the formation of higher C containing species derived from propylene, either coke or aromatics (Table 2). Comparing the performance of Gaδ+ Pt0 /SiO2 to each of the monometallic systems, GaIII/SiO2 and Pt0 /SiO2, tested at lower WHSVs (10 mL/min; 20% C3H8 in Ar; WHSV, 2.1 h−1) with conversions below equilibrium indicated a dramatic improvement of catalytic performance for the bimetallic system. For comparison, the Pt0 /SiO2 catalyst operates with an initial conversion of 19.0%, albeit with low propylene selectivity (59.2%) and relatively fast deactivation over a 2 h period (kd = 1.0), which is typical of unmodified and supported Pt nanoparticles.2 In contrast, GaIII/SiO2 exhibits high propylene selectivity (94.0%) at conversions of 9.3% under similar catalytic conditions. Over 20 h of catalysis, GaIII/SiO2 showed minimal deactivation (kd = 0.02) in comparison to Pt0 /SiO2. The higher WHSV at which Gaδ+ Pt0 /SiO2 maintains high conversions and selectivity indicates a significantly greater propylene productivity (31.5 g C3H6 g cat−1 h−1) when compared to the monometallic systems Pt0 /SiO2 (0.24 g C3H6 g cat−1 h−1) and GaIII/SiO2 (0.16 g C3H6 g cat−1 h−1). The initial productivity reported in the literature for other GaxPty/ Al2O3 systems, prepared through sequential impregnation methods and reduction, is significantly lower and ranges from ca. 2−4gC3H6 g cat−1 h−1 despite operating at considerably higher reaction

temperatures (≥600 °C).10,11 Other systems based on modified hydrotalcites, GaxPty/Mg(Ga)(Al)O, have been reported with similarly low initial productivity, which can be increased up to 11.6 g C3H6 g cat−1 h−1 while cofeeding 1.25 mol equiv of H2 with respect to C3H8; 15,16,18 a condition that typically increases stability and activity rates by up to an order of magnitude.16,48,49 The high productivity of Gaδ+ Pt0 / SiO2, when compared to other Ga−Pt systems, in the absence of H2 is noteworthy and can be attributed to the ability of SOMC to access nanometric alloyed particles at higher metal loadings in comparison to other synthetic strategies that generate larger nanoparticles at significantly lower platinum loadings. In addition to the high initial propylene productivity, Gaδ+ Pt0 /SiO2 presents unusual long-term stability reaching a productivity of 17.1 g C3H6 g cat−1 h−1 after 20 h of time on stream. This productivity surpasses the initial activity of other Ga−Pt systems, which have notably shorter catalytic lifetimes (≤2 h).9,10,15,16 To investigate the structural stability of the Gaδ+ Pt0 /SiO2 system during PDH, additional in situ XAS measurements were performed. Under catalytic conditions, no changes in the XANES spectra at the Ga K-edge or Pt L3-edge were evident, indicating minimal change of the catalyst structure over the duration of the XAS measurements (6 h). This differs from similar studies performed on GaIII/SiO2 during PDH, which show the appearance of a new feature at lower energy; this has been attributed to deactivation of gallium single-sites either via reduction or the generation of stable intermediates.24,34,50 These data suggest that deactivation of Gaδ+ Pt0 /SiO2 is likely not attributed to structural change of the catalyst but instead by small amounts of carbonaceous species formed over the duration of the reaction, which is supported by Raman measurements of the spent catalyst displaying vibrational bands characteristic of coke formation (see Supporting Information for details).51 Regeneration of the catalyst was also examined, considering both alloy segregation and removal of coke from the catalyst after PDH. Exposure of the Gaδ+ Pt0 /SiO2 to atmospheric conditions results in dealloying of the GaPt particles, which is supported by XAS measurements (see Supporting Information for details). The dealloyed material was investigated for PDH using a pretreatment in H2 at 500 °C, which resulted in a catalyst with nearly identical catalytic performance in PDH as the initial Gaδ+ Pt0 /SiO2 material. These studies suggest that dealloying of the material under atmospheric conditions is a reversible

process and does not affect the performance of the catalyst. Regeneration of the spent catalyst was also performed through treatment using a flow consisting of 1% O2/Ar (10 mL/min) at 500 °C for 1 h followed by a reduction step (H2, 10 mL/min) to reform the Gaδ+ Pt0 /SiO2 catalyst. Subsequent PDH studies show that the regeneration process returns the catalyst to ca. 75% of the initial activity while maintaining high propylene selectivity (>99%). The combined high activity, selectivity, and stability of Gaδ+ Pt0 /SiO2 is unprecedented and illustrates SOMC's ability in generating unique catalyst features; in this instance, the formation of small alloyed nanoparticles supported on silica containing isolated gallium sites was accomplished.

In summary, we have shown that SOMC is a powerful approach to generate supported nanometric alloyed Ga−Pt particles on silica containing isolated gallium sites. A detailed characterization, including XPS and in situ XAS, shows that the reduced material possesses small GaxPt ($0.5 < x < 0.9$) alloyed nanoparticles with a fraction of the gallium remaining as singlesites. The material shows unprecedented productivity and stability for Ga−Pt systems in PDH. The high activity and selectivity is attributed to SOMC's ability of incorporating significant amounts of active metal at the surface while maintaining small particle size with segregated platinum sites. This feature likely originates from the presence of strong Lewis acid sites remaining at the surface that helps in the nucleation and stabilization of nanometric particles. We are currently exploring this synthetic strategy as a means to open new avenues in the preparation of other catalytic systems.

Funding Sources

The authors are grateful to the Swiss National Foundation (SNF) for financial support of this work (grant no. 200020_149704). K.S. thanks the ETH Career Seed Grant SEED-15 17-1.

ACKNOWLEDGMENTS

We acknowledge the Paul Scherrer Institut, Villigen, Switzerland for provision of synchrotron radiation beam time at beamline Super XAS (proposal #20170700) of the SLS and would like to thank Dr. Maarten Nachtegaal for assistance.

REFERENCES

(1) Malakoff, D. Science 2014, 344, 1464−1467.

(2) Sattler, J. J. H. B.; Ruiz-Martinez, J.; Santillan-Jimenez, E.; Weckhuysen, B. M. Chem. Rev. 2014, 114, 10613−10653.

(3) Nawaz, Z. Rev. Chem. Eng. 2015, 31, 413−436.

(4) Vora, B. V. Top. Catal. 2012, 55, 1297−1308.

(5) Bhasin, M. M.; McCain, J. H.; Vora, B. V.; Imai, T.; Pujado, P. R.́ Appl. Catal., A 2001, 221, 397−419.

(6) Sanfilippo, D.; Miracca, I. Catal. Today 2006, 111, 133−139.

(7) Coperet, C.; Estes, D. P.; Larmier, K.; Searles, K.́ Chem. Rev. 2016, 116, 8463−8505.

(8) Coperet, C.́ Chem. Rev. 2010, 110, 656−680.

(9) Jablonski, E. L.; Castro, A. A.; Scelza, O. A.; de Miguel, S. R. Appl. Catal., A 1999, 183, 189−198.

(10) Sattler, J. J. H. B.; Gonzalez-Jimenez, I. D.; Luo, L.; Stears, B. A.; Malek, A.; Barton, D. G.; Kilos, B. A.; Kaminsky, M. P.; Verhoeven, T. W. G. M.; Koers, E. J.; Baldus, M.; Weckhuysen, B. M. Angew. Chem., Int. Ed. 2014, 53, 9251−9256.

(11) Wang, T.; Jiang, F.; Liu, G.; Zeng, L.; Zhao, Z. j.; Gong, J. AIChE J. 2016, 62, 4365−4376.

(12) Iezzi, R.; Bartolini, A.; Buonomo, F. US Patent 0198428, 2002.

(13) Filez, M.; Redekop, E. A.; Galvita, V. V.; Poelman, H.; Meledina, M.; Turner, S.; Van Tendeloo, G.; Bell, A. T.; Marin, G. B. Phys. Chem. Chem. Phys. 2016, 18, 3234−3243.

(14) Filez, M.; Redekop, E. A.; Poelman, H.; Galvita, V. V.; Ramachandran, R. K.; Dendooven, J.; Detavernier, C.; Marin, G. B. Chem. Mater. 2014, 26, 5936−5949.

(15) Redekop, E. A.; Galvita, V. V.; Poelman, H.; Bliznuk, V.; Detavernier, C.; Marin, G. B. ACS Catal. 2014, 4, 1812−1824.

(16) Siddiqi, G.; Sun, P.; Galvita, V.; Bell, A. T. J. Catal. 2010, 274, 200−206.

(17) Sun, P.; Siddiqi, G.; Chi, M.; Bell, A. T. J. Catal. 2010, 274, 192−199.

(18) Belskaya, O. B.; Stepanova, L. N.; Gulyaeva, T. I.; Leont'eva, N. N.; Zaikovskii, V. I.; Salanov, A. N.; Likholobov, V. A. Kinet. Catal. 2016, 57, 546−556.

(19) Zhou, Y.; Davis, S. M. US Patent 5214227, 1993.

(20) Schweitzer, N. M.; Hu, B.; Das, U.; Kim, H.; Greeley, J.; Curtiss, L. A.; Stair, P. C.; Miller, J. T.; Hock, A. S. ACS Catal. 2014, 4, 1091−1098.

(21) Hu, B.; Getsoian, A.; Schweitzer, N. M.; Das, U.; Kim, H.; Niklas, J.; Poluektov, O.; Curtiss, L. A.; Stair, P. C.; Miller, J. T.; Hock, A. S. J. Catal. 2015, 322, 24−37.

(22) Hu, B.; Schweitzer, N. M.; Zhang, G.; Kraft, S. J.; Childers, D. J.; Lanci, M. P.; Miller, J. T.; Hock, A. S. ACS Catal. 2015, 5, 3494− 3503.

(23) Camacho-Bunquin, J.; Shou, H.; Aich, P.; Beaulieu, D. R.; Klotzsch, H.; Bachman, S.; Marshall, C. L.; Hock, A.; Stair, P. Rev. Sci. Instrum. 2015, 86, 084103.

(24) Getsoian, A.; Das, U.; Camacho-Bunquin, J.; Zhang, G.; Gallagher, J. R.; Cheah, S.; Schaidle, J. A.; Ruddy, D. A.; Hensley, J. E.; Krause, T. R.; Curtiss, L. A.; Miller, J. T.; Hock, A. S. Catal. Sci. Technol. 2016, 6, 6339−6353.

(25) Coperet, C.; Chabanas, M.; Petroff Saint-Arroman, R.; Basset, J.´ M. Angew. Chem., Int. Ed. 2003, 42, 156−181.

(26) Wegener, S. L.; Marks, T. J.; Stair, P. C. Acc. Chem. Res. 2012, 45, 206−214.

(27) Coperet, C.; Comas-Vives, A.; Conley, M. P.; Estes, D. P.;´ Fedorov, A.; Mougel, V.; Nagae, H.; Nuñez-Zarur, F.; Zhizhko, P. A. Chem. Rev. 2016, 116, 323−421.

(28) Pelletier, J. D. A.; Basset, J.-M. Acc. Chem. Res. 2016, 49, 664− 677.

(29) Coperet, C.; Allouche, F.; Chan, K. W.; Conley, M. P.; Delley,´ M. F.; Fedorov, A.; Moroz, I. B.; Mougel, V.; Pucino, M.; Searles, K.; Yamamoto, K.; Zhizhko, P. A. Angew. Chem., Int. Ed. 2018, 57, 6398− 6440.

(30) Fujdala, K. L.; Tilley, T. D. J. Catal. 2003, 216, 265−275.

(31) Conley, M. P.; Delley, M. F.; Nuñez-Zarur, F.; Comas-Vives, A.; Coperet, C.´ Inorg. Chem. 2015, 54, 5065−5078.

(32) Delley, M. F.; Nuñez-Zarur, F.; Conley, M. P.; Comas-Vives, A.; Siddiqi, G.; Norsic, S.; Monteil, V.; Safonova, O. V.; Coperet, C. P.´ Proc. Natl. Acad. Sci. U. S. A. 2014, 111, 11624−11629.

(33) Estes, D. P.; Siddiqi, G.; Allouche, F.; Kovtunov, K. V.; Safonova, O. V.; Trigub, A. L.; Koptyug, I. V.; Coperet, C.´ J. Am. Chem. Soc. 2016, 138, 14987−14997.

(34) Searles, K.; Siddiqi, G.; Safonova, O. V.; Coperet, C.´ Chem. Sci. 2017, 8, 2661−2666.

(35) Camacho-Bunquin, J.; Ferrandon, M.; Sohn, H.; Yang, D.; Liu, C.; Ignacio-de Leon, P. A.; Perras, F. A.; Pruski, M.; Stair, P. C.; Delferro, M. J. Am. Chem. Soc. 2018, 140, 3940−3951.

(36) Ma, Z.; Wu, Z.; Miller, J. T. Catal., Struc. React. 2017, 3, 43−53.

(37) Valla, M.; Stadler, D.; Mougel, V.; Coperet, C.´ Angew. Chem., Int. Ed. 2016, 55, 1124−1127.

(38) Liu, D.; Li, Y.; Kottwitz, M.; Yan, B.; Yao, S.; Gamalski, A.; Grolimund, D.; Safonova, O. V.; Nachtegaal, M.; Chen, J. G.; Stach, E. A.; Nuzzo, R. G.; Frenkel, A. I. ACS Catal. 2018, 8, 4120−4131.

(39) Lam, E.; Larmier, K.; Wolf, P.; Tada, S.; Safonova, O. V.; Coperet, C.´ J. Am. Chem. Soc. 2018, 140, 10530.

(40) Laurent, P.; Veyre, L.; Thieuleux, C.; Donet, S.; Coperet, C.´ Dalton Trans 2013, 42, 238−248.

(41) Ruddy, D. A.; Jarupatrakorn, J.; Rioux, R. M.; Miller, J. T.; McMurdo, M. J.; McBee, J. L.; Tupper, K. A.; Tilley, T. D. Chem. Mater. 2008, 20, 6517−6527.

(42) Haq, S.; King, D. A. J. Phys. Chem. 1996, 100, 16957−16965.

(43) Grassian, V. H.; Muetterties, E. L. J. Phys. Chem. 1986, 90, 5900−5907.

(44) Johnson, A. L.; Muetterties, E. L.; Stohr, J.; Sette, F. J. Phys. Chem. 1985, 89, 4071−4075.

(45) Yoshida, H.; Nonoyama, S.; Yazawa, Y.; Hattori, T. Phys. Scr. 2005, T115, 813−815.

(46) Hsu, L.-S.; Guo, G. Y.; Denlinger, J. D.; Allen, J. W. Phys. Rev. B: Condens. Matter Mater. Phys. 2001, 63, 155105.

(47) Giedigkeit, R.; Hu, Z.; Grin, Y. XANES study on the intermetallic compounds PdGa and PtGa, two representatives of the FeSi structure. http://hasyweb.desy.de/science/annual_reports/ 2002_report/part1/contrib/41/6974.pdf.

(48) Saerens, S.; Sabbe, M. K.; Galvita, V. V.; Redekop, E. A.; Reyniers, M.-F.; Marin, G. B. ACS Catal. 2017, 7, 7495−7508.

(49) Galvita, V.; Siddiqi, G.; Sun, P.; Bell, A. T. J. Catal. 2010, 271, 209−219.

(50) Cybulskis, V. J.; Pradhan, S. U.; Lovon-Quintana, J. J.; Hock, A.´ S.; Hu, B.; Zhang, G.; Delgass, W. N.; Ribeiro, F. H.; Miller, J. T. Catal. Lett. 2017, 147, 1252−1262.

(51) Sattler, J. J. H. B.; Beale, A. M.; Weckhuysen, B. M. Phys. Chem. Chem. Phys. 2013, 15, 12095−12103.